18th IFHTSE CONGRESS
International Federation for Heat Treatment and Surface Engineering
IFHTSE
ANAIS
PROCEEDINGS
ISSN 1516-392X

SURFACE-LAYER MICROSTRUCTURE CONTROL BY HIGH-FREQUENCY INDUCTION HEATING IN METASTABLE AUSTENITIC STAINLESS STEEL[1]

Toshihiro Tsuchiyama[2]
Takanori Tsurumaru[3]
Koichi Nakashima[4]
Setsuo Takaki[2]
Hirokazu Inaba[5]
Yoshitaka Misaka[6]

Abstract
To suppress hydrogen permeation from environment into cold-worked high strength austenitic stainless steel, the surface heat treatment using high-frequency induction heating was applied to a cord-drawn metastable austenitic stainless steel (Fe-16Cr-10Ni alloy). By this heat treatment, the microstructure in the surface-layer (1mm depth) was controlled to austenite, while the inside of the material was strengthened by a large fraction of deformation-induced martensite. TDS analysis for the cathodically charged specimen revealed that hydrogen permeation was significantly retarded and no diffusible hydrogen existed. These results suggest that hydrogen embrittlement can be avoided by covering the material surface with austenite phase even in cold-worked high strength austenitic stainless steel.
Key words: Austenitic stainless steel; Martensite; High-frequency induction heating; Hydrogen.

[1] *Technical contribution to the 18th IFHTSE Congress - International Federation for Heat Treatment and Surface Engineering, 2010 July 26-30th, Rio de Janeiro, RJ, Brazil.*
[2] *Department of Materials Science and Engineering, Kyushu University, Japan.*
[3] *formerly Graduate student of Engineering, Kyushu University, now at SUMCO Corporation, Japan.*
[4] *formerly Department of Materials Science and Engineering, Kyushu University, now at Steel Research Laboratory, JFE steel Corporation, Japan.*
[5] *Technical Headquarters, NETUREN Co., Ltd., Japan.*
[6] *Fine Techno Center, NETUREN Co., Ltd., Japan.*

1 INTRODUCTION

Austenitic stainless steel is an important material used for hydrogen-related structural objects, such as hydrogen transport pipes, storage tanks, hydrogen station, and so on, because of its high strength and toughness at low temperature with excellent corrosion resistance. However, cold working of austenitic stainless steel often increases its hydrogen embrittlement sensitivity. For example, it was reported that cold working prior to hydrogen charging remarkably enhances the reduction of ductility and acceleration of fatigue crack propagation by hydrogen.[1,2] This is due to deformation-induced martensitic transformation of metastable austenite phase during cold working. The hydrogen embrittlement sensitivity of austenitic stainless steel should be originally low due to the FCC structure with low hydrogen diffusivity, but the deformation-induced martensite has BCC structure with high diffusivity, and therefore, hydrogen permeation becomes easy to occur when martensitic structure is formed in the material and it works as hydrogen diffusion paths.[2] We can avoid the hydrogen embrittlement of materials by using stable austenitic stainless steel such as type 316L instead of metastable austenitic stainless steel represented by type 304. However, that problem would not be solved so simply because the deformation-induced martensite is effective for strengthening of material and plays an important role in weight saving of the structural objects.

To satisfy both demands of hydrogen embrittlement resistance and high strength in metastable austenitic stainless steel, we attempted to control the distribution of deformation-induced martensite in order to prevent the hydrogen permeation: the microstructure in the surface-layer contacted with environment was controlled to austenite, while the inside of the material was strengthened by a large fraction of deformation-induced martensite. Since hydrogen enters into material from the surface, its permeation into material would be retarded if the surface-layer is covered with stable austenitic structure with low hydrogen diffusivity.

Such microstructure control could be realized by surface heat treatment using high-frequency induction heating for severely deformed metastable austenitic steel. In this study, a metastable austenitic stainless steel rod (Fe-16%Cr-10%Ni) was subjected to this process, and then the distribution of martensite through radius direction was clarified by EBSP orientation imaging map and hardness profile. For this specimen, hydrogen permeation behavior was investigated by hydrogen charge followed by thermal desorption spectroscopy (TDS).

2 MATERIALS AND METHODS

Metastable austenitic stainless steel, Fe-16%Cr-10%Ni alloy, was mainly used in this study. In addition, commercial type 304 and 316L austenitic stainless steels were also prepared to evaluate the effect of austenite stability on hydrogen permeation behavior. The detailed chemical composition and Md_{30} temperature of the specimens are shown in Table 1. The Md_{30} temperatures, which represent the stability of each austenite, were calculated with the equation (1) proposed by Angel.[3]

$$Md_{30}\,(K) = 686 - 462\,(C+N) - 9.2Si - 8.1Mn - 13.7Cr - 9.5Ni - 18.5Mo \quad (1)$$

(C, N, Si, Mn, Cr, Ni, Mo : mass%)

Table 1. Chemical compositions of steels used in this study (mass%)

steels	C	Si	Mn	P	S	Cr	Ni	Mo	Fe	Md_{30} (K)
SUS304	0.06	0.50	0.90	0.033	0.007	18.18	8.12	—	bal.	320
SUS316L	0.009	0.47	0.73	0.025	0.001	17.09	12.16	2.84	bal.	269

The 304 and 316L specimens were subjected to solution treatment at 1373K for 1.8ks followed by air cooling, and then cold-rolled at ambient temperature up to 80% in thickness reduction. On the other hand, 16Cr-10Ni steel was produced by vacuum melting, hot forging and swaging, followed by cold drawing from φ24mm to φ7mm (90% in area reduction). It was confirmed that almost all austenite had been transformed to martensite after the cold drawing. The rod specimen obtained was then subjected to surface heat treatment using high-frequency induction heating to 958K to reverse the deformation-induced martensite to austenite in the surface-layer.

The microstructure and the distribution of deformation-induced martensite were investigated with optical microscopy, crystallographic orientation measurement by SEM-EBSD, and X-ray diffractometry. The average amount of deformation-induced martensite was estimated by saturated magnetization measurement. The hydrogen permeation behavior was evaluated by thermal desorption spectroscopy (TDS) for the plate specimens (φ7mm- 1mm thick) dipped in a 20% ammonium thiocyanate solution at 323K for 86.4ks as schematically drawn in Figure 1. For the 16Cr-10Ni steel with austenitic surface-layer, the cut plane was masked with silicon rubber to avoid hydrogen entry from that plane.

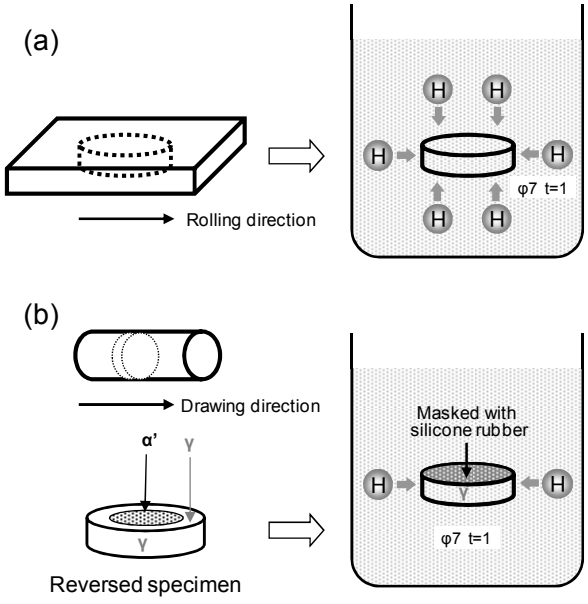

Figure 1. Preparation process of TDS analysis specimens for cold-rolled 304, 316L steels (a) and cold-drawn 16%Cr-10%Ni steel (b).

3 RESULTS AND DISCUSSION

3.1 Effect of Deformation-induced Martensite on Hydrogen Permeation Behavior in Cold-rolled Austenitic Stainless Steels

Figure 2 represents optical micrographs of solution-treated and cold-rolled 304 and 316L stainless steels. Both of the solution-treated specimens exhibit austenitic single structure with a similar grain size of around 50 microns. In the cold-rolled specimens, streaky deformation structure is observed within the elongated austenite grains. However, it is impossible to distinguish deformation-induced martensite from deformed austenitic structure such as deformation bands and deformation twins in these optical micrographs.

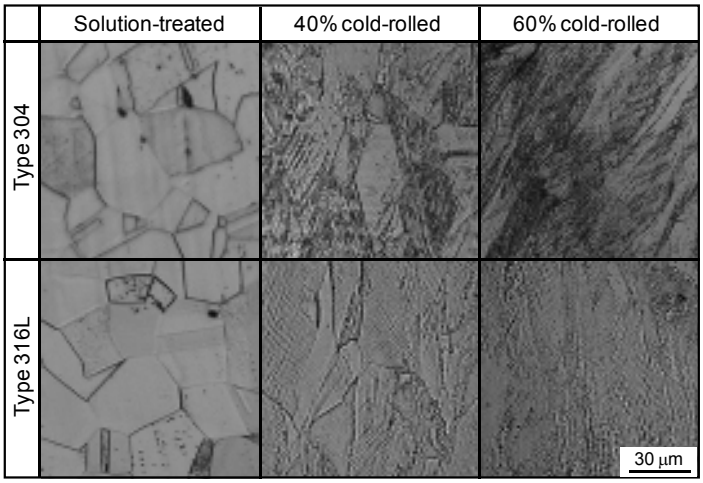

Figure 2. Optical micrographs of solution-treated and cold-rolled 304 and 316L steels.

Figure 3 shows changes in Vickers hardness and volume fraction of martensite in cold-rolled 304 and 316L stainless steels as a function of thickness reduction by cold rolling. Hardness increases with increasing the thickness reduction in both steels, but the hardening rate is different between the steels: 304 steel is more rapidly hardened than 316L steel. This suggests that 316L steel is strengthened only by work hardening due to dislocations introduced into austenite, while 304 steel is done by not only work hardening of austenite but also a large amount of deformation-induced martensite formed during cold rolling. The distribution of martensite in a cross section of cold-rolled 304 stainless steel plate is revealed in Figure 4 with crystal orientation map obtained by SEM-EBSD method. The smooth gray area in this map corresponds to austenite that did not transformed to martensite during the cold rolling, while the sandy black area (undetected zone) indicates the distribution of deformation-induced martensite. The martensite is dispersed in the whole of specimens, but tends to be frequently formed near grain boundaries and specimen surface. It should be noted that almost all the specimen surface is covered with martensite. We can imagine that if such material is exposed in a hydrogen existing environment, hydrogen would rapidly permeate the martensite formed on the surface and enter inside of the material, and while if the surface-layer was controlled to austenite, the hydrogen permeation would be effectively suppressed.

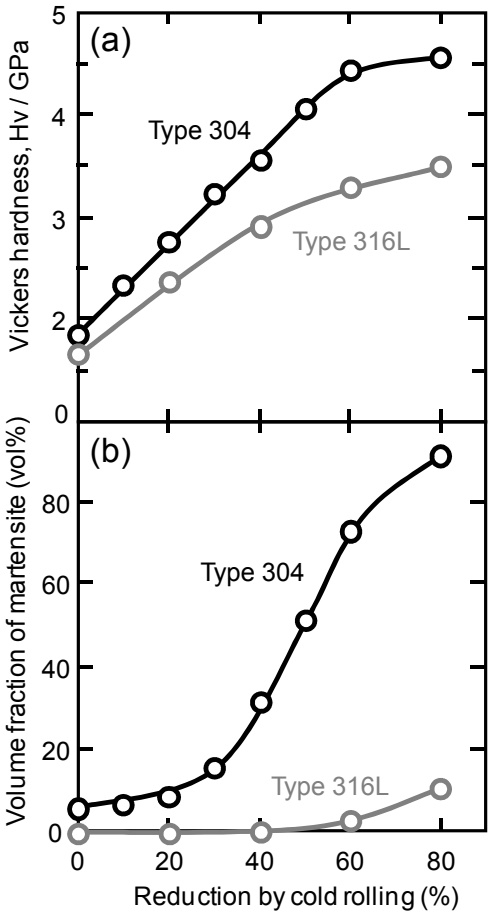

Figure 3. Changes in Vickers hardness (a) and volume fraction of martensite (b) in cold-rolled 304 and 316L steels as a function of thickness reduction by cold rolling.

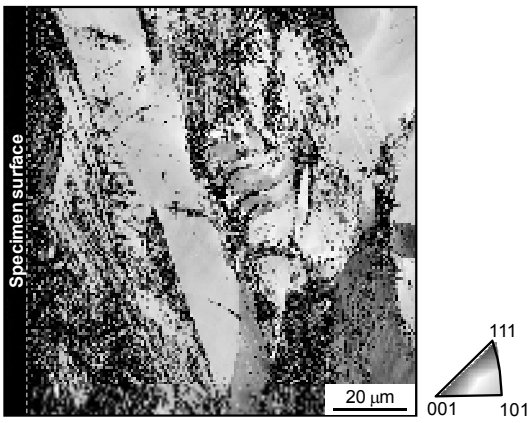

Figure 4. Crystal orientation map showing distribution of deformation-induced martensite in 40% cold-rolled 304 steel.

Firstly, the relation between volume fraction of martensite and amount of hydrogen absorbed into steel was investigated without taking the distribution of martensite into consideration. Figure 5 shows TDS hydrogen desorption curves for the 316L and 304 stainless steels with different cold rolling reduction where the deformation-induced martensite is uniformly distributed. Hydrogen was charged by dipping specimens in a 20% ammonium thiocyanate solution at 323K for 86.4ks. A small peak is observed at around 650K in each of the 316L steels including solution-treated specimen. It is found that there is no significant effect of cold rolling on the hydrogen desorption behavior in this case. On the other hand, the 304 steels exhibit another peak at around 450K in addition to the 650K peak. The hydrogen desorbed at the lower temperature corresponds to the hydrogen atoms which had been weakly trapped by lattice defects such as dislocations and vacancies,[4] and that is generally called 'diffusible hydrogen'. It is known that hydrogen embrittlement of steel is enhanced through the aggregation of diffusible hydrogen atoms to the crack tip.[2,4]

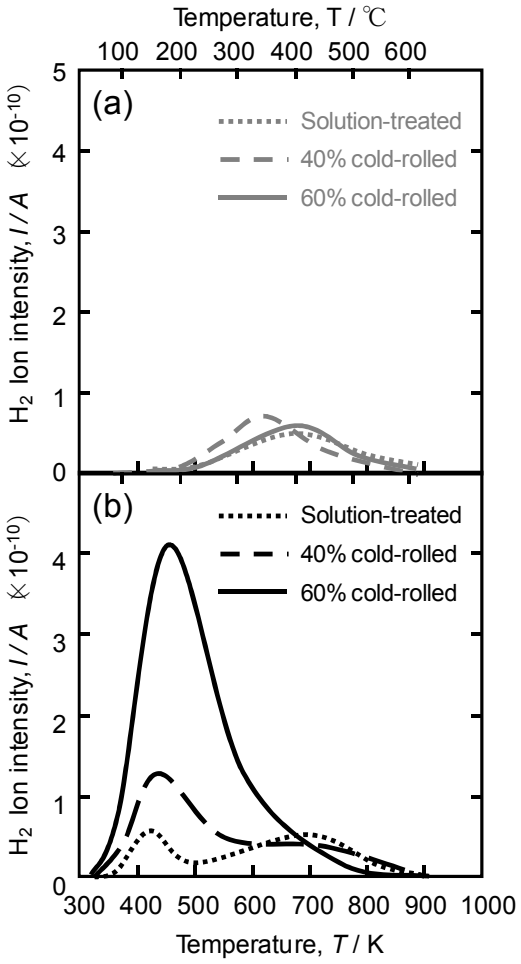

Figure 5. Changes in hydrogen desorption curves in 316L (a) and 304 (b) steels as a function of temperature.

Figure 6 shows relation between average hydrogen content and thickness reduction by cold rolling in the 316L and 304 specimens estimated from the hydrogen desorption curves. The volume fraction of martensite of each specimen is also shown in this figure.

In the 316L specimens in which martensite is not formed, the absorbed hydrogen content hardly changed even after cold rolling, while in the case of 304 specimens, the amount of hydrogen is markedly increased with increasing volume fraction of martensite induced by cold rolling. It is obvious that the amount of absorbed hydrogen is directly related with that of deformation-induced martensite, suggesting the martensite dispersed within austenite matrix works as a diffusion path or existing sites of hydrogen atoms in steels.

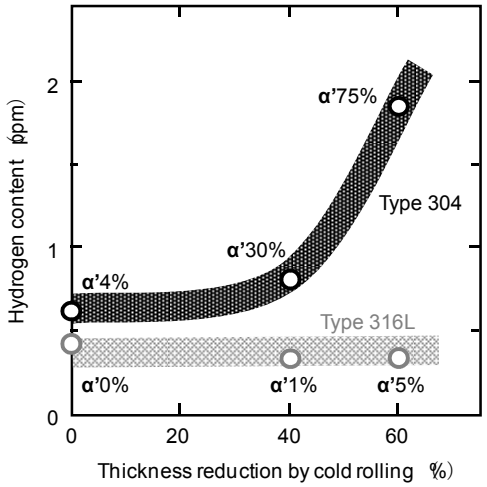

Figure 6. Relation between average absorbed hydrogen content and thickness reduction by cold rolling in 304 and 316L steels.

3.2 Effect of Austenitic Surface-layer on Hydrogen Permeation Behavior

The experimental results mentioned above have demonstrated that deformation-induced martensite enhances the hydrogen permeation into stainless steel. However, that is true under the condition that martensite is uniformly distributed in the specimens. Since hydrogen enters into material from the surface contacted with the atmosphere, not only the amount of martensite but also its distribution should be also important to understand the hydrogen permeation behavior. If the martensite is mainly located inside of the material while the surface-layer is covered with stable austenitic structure, it is expected that hydrogen permeation is significantly retarded even when the average volume fraction of martensite is large. To prove this idea, a thermomechanical treatment shown in Figure 7 was applied to 16Cr-10Ni steel. The rod specimen with full martensitic structure was obtained by cold drawing, and then it was subjected to high-frequency induction heating to reverse the surface-layer of martensite to austenite. Figure 8 represents a macroscopic picture of longitudinal section of specimen and the hardness distribution on the section as a function of the distance from surface. The contrast appeared by polishing and etching in the picture indicates the microstructural change has occurred in the surface-layer of the specimen. The hardness is also discontinuously varied corresponding to the change of microstructure, revealing that the surface-layer of 1mm thick has been altered by induction heat treatment. Figure 9 shows X-ray diffraction patterns obtained from the center part of specimen (a) and the surface-layer (b). The surface-layer of 1mm thick mainly consists of the reversed austenitic structure, while full martensitic structure still remains inside of the layer.

Microstructure observation with SEM-EBSD revealed that the fine-grained austenitic structure with a grain size of around 3 microns had been formed in the surface-layer.

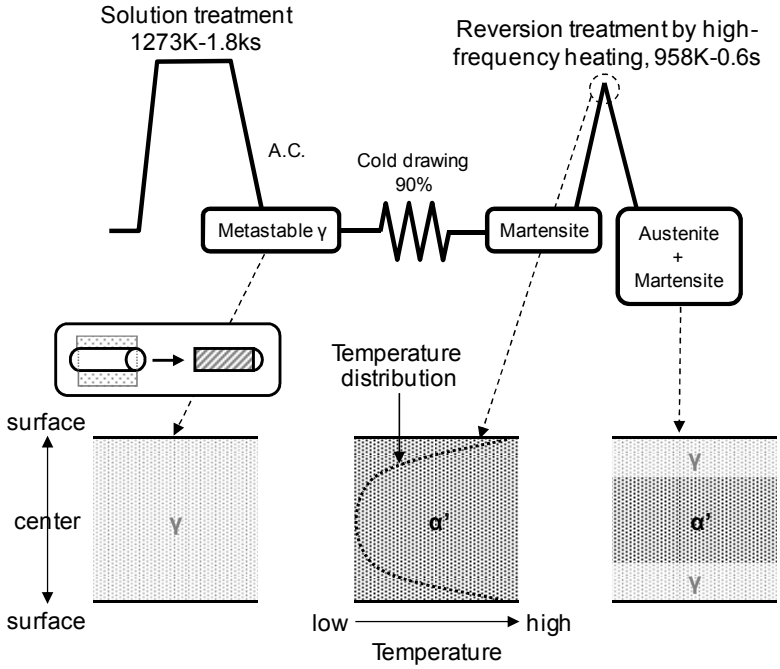

Figure 7. Schematic illustration showing thermomechanical treatment for surface-layer microstructure control.

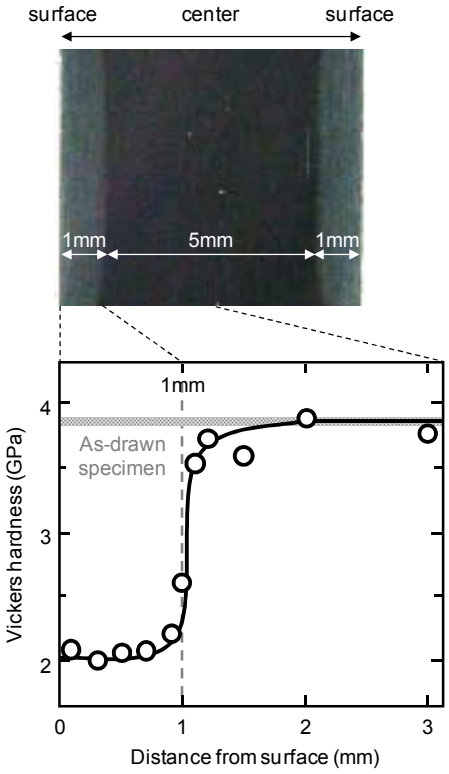

Figure 8. Macroscopic picture of longitudinal section and hardness distribution on the section as a function of the distance from surface in 16%Cr-10%Ni steel subjected to high-frequency induction heating.

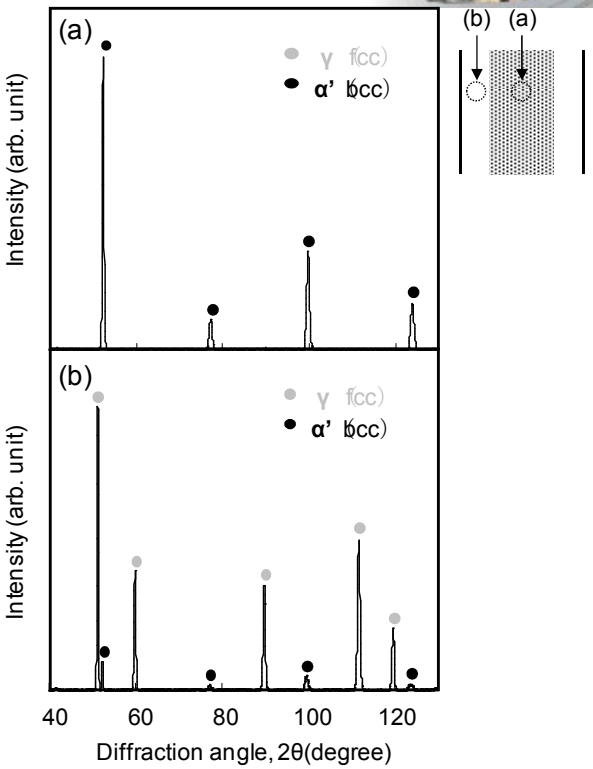

Figure 9. X-ray diffraction patterns obtained from center part of specimen (a) and surface-layer (b) in induction heat-treated 16%Cr-10%Ni steel.

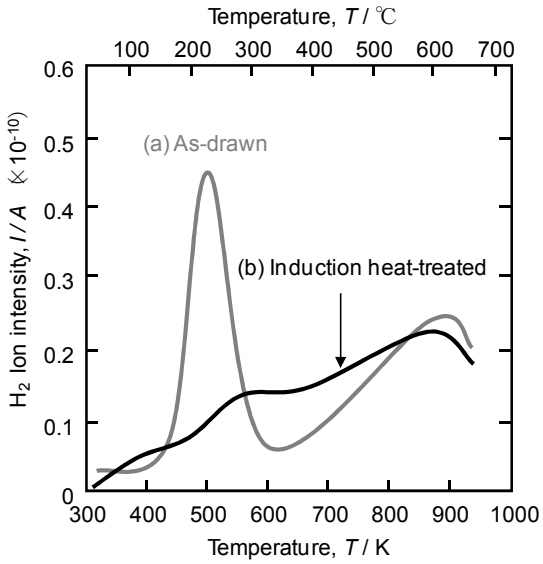

Figure 10. Hydrogen desorption curves of as-drawn (a) and induction heat-treated (b) 16%Cr-10%Ni steels.

Hydrogen permeation behavior for the induction heat-treated specimen with austenitic surface-layer was investigated by hydrogen charging and TDS analysis, as shown in Figure 10. In the as-drawn specimen, significantly large peak is detected at around 500K, which corresponds to the harmful diffusible hydrogen. On the other hand, no peak of diffusible hydrogen is observed in the induction heat-treated specimen.

This indicates that the austenitic surface-layer prevent the hydrogen permeation. In other words, it would be possible to utilize high strength metastable austenitic stainless steel as a structural material in a hydrogen environment if the surface-layer of the material could be controlled to austenite by means of high-frequency induction heating.

4 CONCLUSIONS

(1) In type 304 stainless steel with metastable austenitic structure, the amount of hydrogen absorbed from ammonium thiocyanate solution is increased with increasing the reduction by cold rolling, while in type 316L stainless steel with stable austenitic structure, the amount of absorbed hydrogen is hardly influenced by cold rolling.

(2) Austenitic surface-layer with fine-grained structure can be formed by surface heat treatment using high-frequency induction heating in cold-worked metastable austenitic stainless steel.

(3) Hydrogen permeation is effectively suppressed by the austenitic surface-layer in spite of the existence of a large amount of deformation-induced martensite inside of the steel. This is due to the much lower diffusivity of hydrogen in austenite compared to that in martensite.

(4) Hydrogen embrittlement resistant of austenitic stainless steel can be improved without enhancing austenite stability. By cutting off the hydrogen diffusion path from the environment at austenitic surface-layer, high strength metastable austenitic stainless steel such as type 304 could be applied as a material for hydrogen-related structural objects.

REFERENCES

1 C. Pan, W. Y. Chu, Z. B. Li, D. T. Liang, Y. J. Su, K. W. Gao and L. J. Qiao: Mater. Sci. Eng. A, A351 (2003), p. 293.
2 T. Kanezaki, C. Narazaki, S. Matsuoka and Y. Murakami: Int. J. Hydrogen Energy, 33 (2008), p. 2604.
3 T. Angel: J. Iron Steel Inst., 177 (1954) , p. 165.
4 K. Takai and R. Watanuki: ISIJ Int., 43 (2003), p. 520.